Transition Metal Ion Directed Self-Assembly of Polynuclear Coordination Complexes: Structural Characterization and Magnetic Properties

Yongli Wei,[a] Hongwei Hou,*[a] Yaoting Fan,[a] and Yu Zhu[a]

Keywords: Magnetic properties / Multidentate ligands / Organic-inorganic hybrid composites / Self-assembly / Transition metals

The reactions of different transition metals with the multidentate ligand *N*,*N*′-bis(1,3,4-thiadiazol-2-yl)-2,6-pyridinedicarboxamide (btapca) afford six new polynuclear complexes: the hexanuclear complexes [{$Zn_6(O)_2(btapca)_4$}·3DMF·2H_2O] (**1**) and [{$Zn_6(O)_2(btapca)_4$}·DMF·MeOH·H_2O] (**2**); the pentanuclear complexes [{$Zn_5(OH)_2(btapca)_4$}·4DMF·H_2O] (**3**), [{$Co_5(OH)_2(btapca)_4$}·4DMF·MeOH·H_2O] (**4**) and [{$Ni_5(OH)_2(btapca)_4$}·4DMF·MeOH] (**5**); and the trinuclear complex [{$Fe_3(OH)(btapca)_3$}·2DMF·2MeOH] (**6**). The dominant characteristic of these polynuclear complexes is that there are μ_3- or μ_4-oxygen atoms in the metal polyhedrons. The hexanuclear complexes **1** and **2** show similar octahedral features based on zinc centers. The five metal centers in complexes **3**, **4** and **5** arrange into two triangles with one common vertex. As for complex **6**, three iron(II)/iron(III) atoms form a plane with a μ_3-OH^- in the center. We also report the magnetic properties of complexes **4**, **5** and **6**. Complex **4** exhibits intramolecular antiferromagnetic exchange, while the analogous complex **5** is dominated by very strong intramolecular ferromagnetic coupling. The trinuclear complex [{$Fe_3(OH)(btapca)_3$}·2DMF·2MeOH] (**6**) shows comparable weak antiferromagnetic coupling.

Introduction

"Self-assembly", defined by Whitesides as "the spontaneous assembly of molecules into structured, stable, noncovalently joined aggregates",[1] was borrowed from biology and since then has been widely used in modern coordination chemistry.[2] In traditional studies of supramolecular self-assembly, hydrogen bonds are most frequently employed, as they are in all biological systems.[3] In recent years, strong metal−ligand interactions in supramolecular architectures aroused great interest. Consequently, the self-assembly of organic ligands and inorganic metal ions became one of the most efficient and widely utilized approaches to the construction of organic/inorganic coordination superarchitectures,[4] which have intriguing properties induced by direct or indirect M−M interactions or a consequence of the positioning and identity of the coordination pockets within the ligand and the ability of metal ion to read these sites in terms of its own coordination algorithms.[5] Thus, such architectures exhibit potential applications in catalysis, electrical conductivity, molecular-based magnets, and host-guest chemistry,[6] and can be exploitated for the design of new materials with desirable properties and the manufacturing of devices and molecular machinery.[7−9]

Thus far, various sophisticated supramolecules have been constructed by self-assembly, such as squares, helices, metallacoronates, cages, capsules, tubes, cylinders, and many high-dimensional structures.[3a,10−17] Amongst these diverse architectures, polynuclear metal clusters have attracted much attention.[18−20] For the preparation of such architectures, well-designed organic ligands with the appropriate choice of donors and bridging groups have become the focus of a great deal of research work. It is well-known that polypyridyl groups have been very useful as programmed components in self-assembly processes,[21] and many polypyridyl ligands have been proved to be very useful in the construction of polynuclear complexes. For example, the alkoxy-diazine ligands have produced a series of high-nuclearity complexes;[5] the pendent-arm ligand 1,4,7-tris-(acetophenoneoxime)-1,4,7-triazacyclononane has resulted in the formation of Cu^{II}, $Co^{II,III}$, Ni_4^{II}, and $Mn_3^{II,III}$ complexes;[22] the bis-chelating ligand 1,2-bis(2,2′-bipyridine-6-yl)ethane has afforded a number of Mn complexes.[18] In most cases, combining with the chelating ligands, oxide bridges are always dominant in these polynuclear species, and they enhance the superexchange between paramagnetic metal ions. Chemists have also paid a great deal of attention to magnetic properties in addition to the versatile structures,[23] and have found that such complexes exhibit unusual supramolecular magnetic properties.[18,22,24−30]

In recent years, our group has been engaged in the study of functional coordination complexes, including polymers[31−34] and polynuclear complexes.[35,36] The design

[a] Department of Chemistry, Zhengzhou University, Henan 450052, P. R. China
Fax: (internat.) + 86-371-776-1744
E-mail: houhongw@zzu.edu.cn

  DOI: 10.1002/ejic.200400110

of ideal multifunctional ligands is one of our main themes. In this context, we prepared the ligand *N*,*N*′-bis(1,3,4-thiadiazol-2-yl)-2,6-pyridinedicarboxamide (btapca) and explored its coordination properties. We found that it can produce different polynuclear complexes when reacted with different metal ions: the hexanuclear complexes $[\{Zn_6(O)_2(btapca)_4\}\cdot 3DMF\cdot 2H_2O]$ (**1**) and $[\{Zn_6(O)_2(btapca)_4\}\cdot DMF\cdot MeOH\cdot H_2O]$ (**2**); the pentanuclear complexes $[\{Zn_5(OH)_2(btapca)_4\}\cdot 4DMF\cdot H_2O]$ (**3**), $[\{Co_5(OH)_2(btapca)_4\}\cdot 4DMF\cdot MeOH\cdot H_2O]$ (**4**) and $[\{Ni_5(OH)_2(btapca)_4\}\cdot 4DMF\cdot MeOH]$ (**5**); and the trinuclear complex $[\{Fe_3(OH)(btapca)_3\}\cdot 2DMF\cdot 2MeOH]$ (**6**). The magnetic properties of complexes **4**, **5**, and **6** are also reported here. The occurrence of indirect metal−metal interactions and metal-oxygen-metal bridging functions leads to dominant magnetic superexchange interactions.

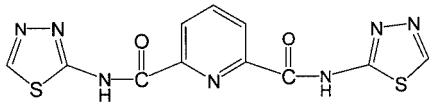

btapca

Results and Discussion

Synthesis

Complexes **1**−**6** were synthesized by the reaction of *N*,*N*′-bis(1,3,4-thiadiazol-2-yl)-2,6-pyridinedicarboxamide (btapca) with different metal salts MX_2 (M = Zn^{II}, Co^{II}, Ni^{II}, Fe^{II}; X = NO_3, OAc, Cl, I) in methanol and DMF solution.

The reaction of $Zn(NO_3)_2\cdot 6H_2O$ with btapca in methanol and DMF (1:1) yielded the hexanuclear complex $[\{Zn_6(O)_2(btapca)_4\}\cdot 3DMF\cdot 2H_2O]$ (**1**). Replacement of $Zn(NO_3)_2\cdot 6H_2O$ with $Zn(OAc)_2\cdot 2H_2O$ in the above reaction led to the related hexanuclear complex $[\{Zn_6(O)_2(btapca)_4\}\cdot DMF\cdot MeOH\cdot H_2O]$ (**2**), which crystallized in a different crystal system and space group to those of complex **1**. In contrast to complexes **1** and **2**, we found that the reaction of ZnI_2 with btapca in a mixture of THF and DMF (1:1) did not afford the hexanuclear complex, but gave the pentanuclear complex $[\{Zn_5(OH)_2(btapca)_4\}\cdot 4DMF\cdot H_2O]$ (**3**) instead, which exhibits a "bow-tie" backbone. Interestingly, we also obtained pentanuclear complexes $[\{Co_5(OH)_2(btapca)_4\}\cdot 4DMF\cdot MeOH\cdot H_2O]$ (**4**) and $[\{Ni_5(OH)_2(btapca)_4\}\cdot 4DMF\cdot MeOH]$ (**5**) in the presence of $CoCl_2\cdot 6H_2O$ and $Ni(NO_3)_2\cdot 6H_2O$, respectively, their structures are similar to that of complex **3**. The reaction of $FeCl_2\cdot 4H_2O$ with btapca led to the trinuclear complex $[\{Fe_3(OH)(btapca)_3\}\cdot 2DMF\cdot 2MeOH]$ (**6**), which has a planar unit completely different from the structures of the other five complexes.

The following chart illustrates the syntheses and structural relationships based on the above discussions.

Crystal Structure of $[\{Zn_6(O)_2(btapca)_4\}\cdot 3DMF\cdot 2H_2O]$ (1)

The crystal structure of complex **1** is illustrated in Figure 1. In the structure, there are six Zn^{II} ions bound by four ligands in the available coordination polyhedron. These six zinc atoms show two different kinds of coordination environments. The inner Zn(3) and Zn(4) atoms are coordinated in a roughly tetrahedral fashion, with two N atoms from different btapca ligands, and O(9) and O(10). The Zn(3)−N(O) bond lengths lie in a fairly narrow range [1.979(9)−2.022(14) Å], and the N−Zn(3)−O angles vary from 109.5° to 117.2°. The corresponding bond lengths and angles around Zn(4) are identical to those of Zn(3), in the range 1.964(9)−2.00(2) Å and 107.7(5)−115.8(5)°, respectively. The Zn(3)···Zn(4) distance is 2.802(2) Å, suggesting that there is a strong interaction between Zn(3) and Zn(4). Such short Zn···Zn distances are unusual in polynuclear zinc complexes.[37−43]

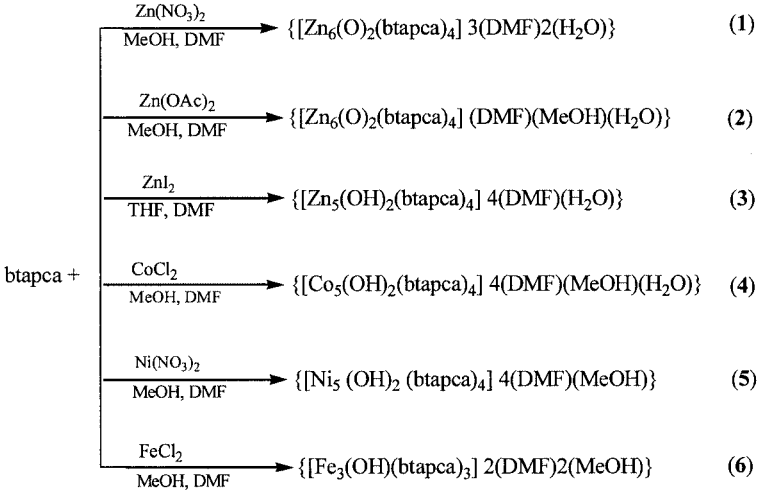

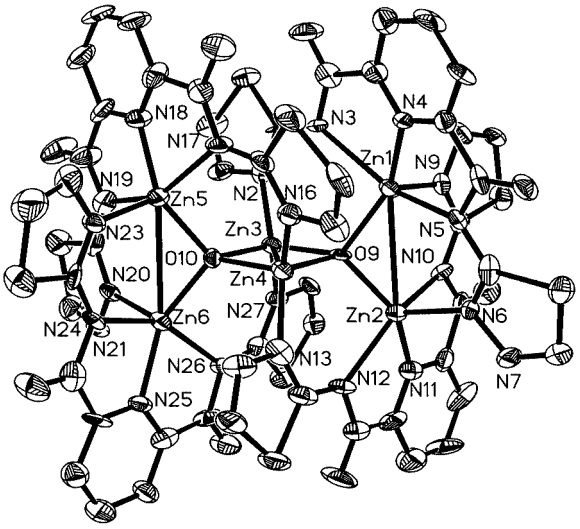

Figure 1. The hexanuclear backbone of $[\{Zn_6(O)_2(btapca)_4\}\cdot 3DMF\cdot 2H_2O]$ (**1**)

The other four zinc atoms Zn(1), Zn(2), Zn(5) and Zn(6) are connected to Zn(3) and Zn(4) through the O(9) and O(10) atoms. All these four Zn atoms are five coordinate and exhibit an approximately tetragonal pyramidal coordination geometry. In the polyhedron of Zn(5), N(17), N(18), N(19), O(10) lie in the basal plane, with a best least-squares deviation of 0.1274 Å, and N(23) occupies the apex. Zn(6) is identical to Zn(5). The slightly longer Zn(1)···Zn(2) [3.129(3) Å] and Zn(5)···Zn(6) [3.144(3) Å] distances suggest weaker interactions between the Zn atoms than Zn(3)···Zn(4), but still show a close Zn···Zn contact compared to those in the literature (falling in the range 3.0−4.4 Å).[37−43]

Considering the six zinc atoms as the symmetry core, the motif can be described as a rough octahedron. There is a pseudo-fourfold axis along Zn(3) and Zn(4). The basal plane is made up of Zn(1), Zn(2), Zn(5) and Zn(6), with a deviation of 0.0540 Å, and the four edges are 3.129, 3.144, 4.995 and 5.161 Å, respectively. Zn(3) and Zn(4) occupy the two apical sites.

The skeleton of **1** can also be described as edge-shared double tetrahedrons. Two isolated oxygen atoms are located in the center of each tetrahedron, and Zn(3)···Zn(4) is the common edge. In the outside of the Zn_6O_2 core, four ligands coil in a tetra-helical style.

The asymmetric unit contains two formula units; all the asymmetric units pack in a three-dimensional fashion based on hydrogen bonding. Along the crystallographic *a* direction, every $[Zn_6(O)_2(btapca)_4]$ unit is linked through O(2)···S(7) and O(2)···H−C(7). O(3)···H−C(33) hydrogen bonds form in the *b* direction, and O(8)···H−C(28) and O(1)···H−C(17) bonds in the *c* direction. All these contacts are weak van der Waals interactions, whose distances are in the range 2.375−3.140 Å. Although these interactions are comparatively weak, they may play a role in the stabilization of the crystal structure. The solvent DMF and H_2O molecules do not influence the structure of $[Zn_6(O)_2(btapca)_4]$, and are dispersed in the spaces of the structure.

Crystal Structure of $[\{Zn_6(O)_2(btapca)_4\}\cdot DMF\cdot MeOH\cdot H_2O]$ (2)

Complex **2** has a different space group from complex **1**, but its crystal structure is similar to that of **1** except for the solvent molecules. The two Zn−N distances are in the ranges 2.020(6)−2.284(6) Å and 1.972(6)−1.996(6) Å, and the Zn−O distances are in the range 1.939(5)−1.989(5) Å, slightly shorter than the corresponding distances in **1**. The shortest Zn···Zn distance is 2.8103 Å, and the longest 3.1456 Å. The asymmetric units also pack in a three-dimensional fashion through hydrogen bonding [O(4)···H(47), O(13)···H(11), O(2)···H(7) and S(6)···H(5)]. The lengths of these hydrogen bonds range from 2.470 to 2.934 Å.

The crystal structures of hexanuclear complexes **1** and **2** are very novel, although various Zn-containing polynuclear complexes have been reported previously. For example, in the hexanuclear zinc(II) cage $[Zn_6Cl_4(3,5\text{-}Me_2PzH)_8(PhPO_3)_4]$ (Me_2PzH = 3,5-dimethylpyrazole), the six zinc centers are arranged in a chair-like conformation.[38] The tetranuclear complex $[Zn_2L(\mu_{1,1}\text{-}HCO_2)(\mu_{1,3}\text{-}HCO_2)]_2(ClO_4)_2$ {L = 2,6-bis[*N*-2-(2′-pyridylethyl)formimidoyl]-4-methylphenol}[37] consists of two identical dinuclear $[Zn_2L(\mu_{1,1}\text{-}HCO_2)(\mu_{1,3}\text{-}HCO_2)]^+$ subunits which connect to each other through an interaction between the dangling oxygen of the formate and the zinc atom of the other subunit. The structure of the trinuclear compound $[Zn_3Cl(3,5\text{-}Me_2Pz)_4(t\text{BuPO}_3)_2]$[38] contains a planar trizinc assembly containing two bicapping $\mu_3[t\text{BuPO}_3]^{2-}$ ligands and terminal pyrazole and chloride ligands. The trinuclear complex $[Zn_3L(NH_3)_3(H_2O)_3]Cl\cdot H_2O$[44] [L = tris(2-hydroxybenzylidene)triaminoguanidine] adopts a propeller-like conformation. The six zinc centers in complexes **1** and **2** arrange in a completely different way, with a roughly octahedral conformation.

Crystal Structure of $[\{Zn_5(OH)_2(btapca)_4\}\cdot 4DMF\cdot H_2O]$ (3)

The pentanuclear backbone is based on a $Zn_5(\mu_3\text{-}OH)_2$ "bow-tie" cluster in which two triangles share one vertex [Zn(2)]. The three edges of each triangle are 3.413, 3.269, 3.269 Å, respectively, making it close to isosceles. The structural unit is illustrated in Figure 2. There is a 4(1)/*n* symmetry axis running through the central Zn(2) atom, and each asymmetric unit contains two formula units.

Zn(1) is six-coordinate by N(3), N(4), N(5), O(3), N(2), N(7) from three ligands. N(3), N(4), N(5) and O(3) comprise the equatorial plane, with a deviation of 0.0622 Å, and N(2) and N(7) occupy the two axial positions. Zn(2) is also in an octahedral coordination environment, with four N atoms in the equatorial plane and two O atoms at the axis. The Zn(2)−O distances fall in the range 1.940(11)−2.041(8) Å. O(3) is located in the mean plane of Zn(1)−Zn(1A)−Zn(2) with a best least-squares deviation of 0.1751 Å. The Zn−O−Zn angles fall in a fairly narrow range [110.4(4)−119.2(6)°]. The Zn−O and Zn−N bond

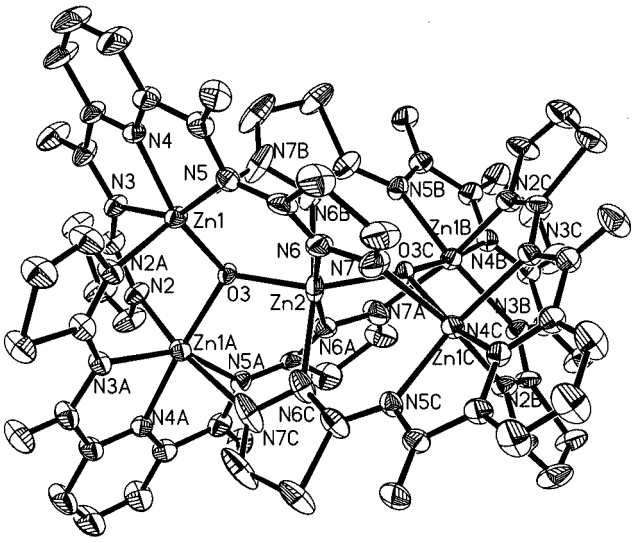

Figure 2. The pentanuclear unit of $[\{Zn_5(OH)_2(btapca)_4\}\cdot 4DMF\cdot H_2O)$ (**3**)

lengths are similar to those reported in the literature,[9,39,40,45–47] which are in the range 1.92–2.42 Å.

Complex **3** has a cage-like skeleton taking into account the hydrogen bonds. The solvent DMF and H_2O molecules are located in the cages and do not take part in the hydrogen bonding. The hydrogen bonds are formed between O(2)···H(1) and O(1)···H(11) with distances of 2.561 and 2.557 Å, respectively; the O(2)···S(1) distance is 3.180 Å, which indicates a weak van der Waals interaction.

Crystal Structure of $[Co_5(OH)_2(btapca)_4]\cdot 4DMF\cdot MeOH\cdot H_2O]$ (4)

The molecular structure of complex **4** is depicted in Figure 3. The pentanuclear backbone is similar to **3**: a 4(1)/*n* symmetry axis runs through the central Co(2) atom and each asymmetric unit contains two formula units. Each triangle has a μ_3-OH at its center and is held together by four peripheral ligands in a manner similar to the polymer $[\{Co_5(OH)_2\{1,2,4,5\text{-}(O_2C)_4C_6H_2\}_2(H_2O)_4\}\cdot xH_2O\}_n$.[48] Five cobalt centers share four ligands. Co(1) is coordinated by three ligands and two oxygens, while Co(2) is bound to four ligands and two oxygens. The two Co_3 triangles, joined through a Co(2) vertex, are almost isosceles, with edges of 3.346, 3.359, 3.359 Å, respectively. The dihedral angle of the two triangles is 90.0°. The longer distances Co(1B)···Co(1A) and Co(1B)···Co(1) are 6.288 Å. Consequently, a virtual S_2 axis through Co(2) atom can be postulated from the Co_5 core. In the tetranuclear $[Co_4O_4(O_2CR)_2(bpy)_4]^{3+}$ (bpy = 2,2′-bipyridine) salts,[49] the Co···Co distances are in the range 2.874(1)–2.641(1) Å; such short Co···Co distances are the result of short bridges formed only by oxygen atoms. On the contrary, the Co···Co distances in the trinuclear cation $[L_2Co_2^{III}Co^{II}]^{2+}$ [H_3L = 1,4,7-tris(acetophenoneoxime)-1,4,7-triazacyclononane][22] are much longer [3.402(2) and 6.805(4) Å, respectively]. Generally, the reported Co···Co distances range from 2.4 Å to 3.5 Å.[50–53] The Co···Co distances in **4** (about 3.3 Å) are in this range.

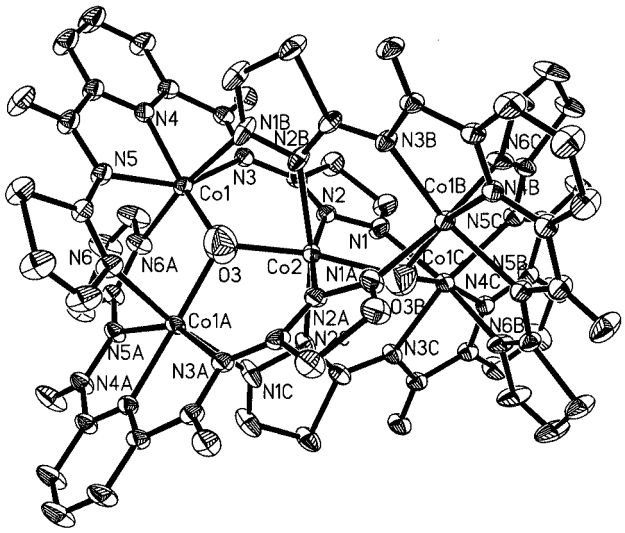

Figure 3. The pentanuclear unit of $[\{Co_5(OH)_2(btapca)_4\}\cdot 4DMF\cdot MeOH\cdot H_2O)$ (**4**) in which two triangles share one common vertex based on cobalt centers

Complex **4** can also be described as four Co(btapca) fragments joined to the Co(2) atom through oxygen bridges. The central Co(2) is bonded by N(2), N(2A), N(2B) and N(2C) from different ligands and two μ_3-O(3) atoms. The four nitrogen atoms from the equatorial plane and the two oxygen atoms occupy the axial positions. The O(3)–Co(2)–O(3B) bond angle of 158.0(3)° is far from the octahedral value of 180°. The Co(2)–O(3) distance [2.021(7) Å] is significantly shorter than the Co–O distance [2.082(3) Å] in the cation $[L_2Co_2^{III}Co^{II}]^{2+}$.[22] This phenomenon is expected for an axially compressed Jahn–Teller ion: "The high-spin Co^{II} ($t_{2g}^5e_g^2$) complexes are susceptible to Jahn–Teller distortions although the structural effect would be expected to be considerably less pronounced, since the degeneracy occurs in the t_{2g} d-orbital set rather than in the e_g set".[22] The antiferromagnetic effect of complex **4** further confirms the high-spin d^7 electronic configuration of the Co centers.

Each Co(1) atom is also in a distorted octahedral environment surrounded by N(3), N(4), N(5), N(6), N(1) and O(3). The Co(1B) atom is located in the mean plane of N(3B)–N(4B)–N(5B)–O(3B) with a deviation of 0.0912 Å. Along the axial direction, the two apical positions are occupied by N(1A) and N(6C), which come from another two ligands. The Co(1)–N(O) distances are in the range 1.998(10)–2.262(5) Å, and are in agreement with the high-spin description of the Co^{II} centers.

All the structural units are loosely packed in line along the *a* axis, and there are only weak O(1)···S(2) (3.228 Å) interactions between every two units. Solvent molecules occupy the space between the units.

Crystal Structure of [{$Ni_5(OH)_2(btapca)_4$}·4DMF·MeOH] (5)

As in the cases of **3** and **4**, the structure of **5** also consists of a pentanuclear [$Ni_5(OH)_2(btapca)_4$], a 4(1)/*n* symmetry axis runs through the central Ni(2) atom, and each asymmetric unit contains two formula units. The structural unit is illustrated in Figure 4. Five Ni^{II} ions are bridged by 24 nitrogen atoms, with four ligands coiling round the [$Ni_5(OH)_2$] core. The distance between two adjacent Ni(1) atoms is 3.444 Å, and the Ni(1)···Ni(2) distances are 3.287 Å. In this point it is similar to **3**, in which the distances between two adjacent Zn(1) atoms are about 3.4 Å, while the Zn(1)···Zn(2) distances are much shorter (about 3.2 Å). The $Ni(1)-N_{(amide)}$ distances fall in the range 2.129(7)−2.151(7) Å, and the $Ni(2)-N_{(thiazole)}$ distances are slightly longer [2.276(7) Å]; the $Ni-N_{(py)}$ distance [1.966(7) Å] is much shorter.

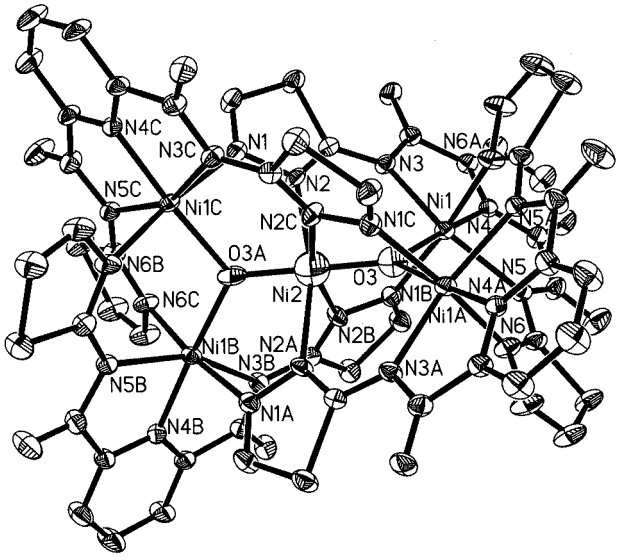

Figure 4. The pentanuclear structure of [{$Ni_5(OH)_2(btapca)_4$}·4DMF·MeOH) (**5**), showing similar feature to those of complex **3** and **4**; the μ_3-OH has been located exactly

The structure of **5** is loosely packed in three dimensions. O(1)···S(2) (3.236 Å) and S(1)···H(7) (2.941 Å) hydrogen bonds are found to connect the whole structure. Channels can be easily seen along the direction perpendicular to the *ac* plane, and the solvent molecules are found in these channels.

Although the skeleton of **5** is similar to those of **3** and **4**, there is a major difference between them. In **3** or **4**, the μ_3-OH is disordered in the center of the M_3 core whereas in **5**, μ_3-OH can be located exactly, with a $Ni(1)-O_{(\mu3)}$ distance of 2.041(6) Å and a $Ni(2)-O_{(\mu3)}$ distance of 1.703(10) Å. The short length of the $Ni(1)-O_{(\mu3)}-Ni(2)$ bridge (about 3.74 Å) leads to active superexchange between the metal ions, as shown by their magnetic-exchange phenomena.

There are many Ni-based complexes with nuclearities ranging from two to eight. The octanuclear ring [$Ni_8(DPKOH\text{-}2H)_4(H_2O)_8](BF_4)_8\cdot 16H_2O$[54] {DPKOH-2H = 1,2-bis[di(pyridin-2-yl)methyleneamino]oxalodiimidic acid}, for example, has a square grouping of six-coordinate Ni^{II} centers arranged in the external ligand pockets. Tetranuclear Ni^{II} complexes are also common,[22,28,29,55−57] for example the [2 × 2] square tetranuclear grid [$Ni_4(POAP\text{-}H)_4(H_2O)_4](NO_3)_4\cdot 8H_2O$ (POAP = alkoxydiazine ligand),[55] the dimer of dimers complex [$Ni_4(ICIMP)_2(Ph_2Ac)_2(urea)(H_2O)][ClO_4]_2$ [56] [ICIMP = 2-{*N*-isopropyl-*N*-[(1-methylimidazolyl)methyl]aminomethyl}-6-{*N*-carboxylmethyl)-*N*-[(1-methylimidazolyl)methyl]aminomethyl}-4-methylphenol], the cation [{$(L^2)Ni_2(\mu\text{-}pydz)(N_3)_2\}_2]^{2+}$ {L^2 = *N*,*N*′-bis[(2-thio-3-aminomethyl-5-*tert*-butylbenzyl)-propane-1,3-diamine]},[57] which contains a rectangular array of four Ni^{II} ions, tetrameric [$Ni_4L_3(H_2O)][ClO_4]_2\cdot 2H_2O$ [H_2L = bis(3-propionyloxy)-1,5-diazacyclooctane],[29] which has a planar triangular Ni_4 topology, the dicubane-like tetramer [Ni(dpk·OH)$(N_3)]_4\cdot 2H_2O$ [dpk = di(2-pyridyl) ketone],[28] and the planar trigonal-shaped tetranuclear Ni^{II} species $[Ni_4(HL)_3]^{2+}$[22] [HL = 1,4,7-tris(acetophenone-oxime)1,4,7-triazacyclononane]. There are also several reported dinuclear nickel(II) complexes,[58−60] while only a limited number of pentanuclear Ni^{II} complexes have been reported, such as the five-membered ring [$Ni_5(bptz)_5(CH_3CN)_{10}][SbF_6]_{10}$ [bptz = 3,6-bis(2-pyridyl)1,2,4,5-tetrazine].[61] As for the pentanuclear Ni^{II} species **5**, its conformation is completely different. The pentanuclear backbone is based on a $Ni_5(\mu_3\text{-}OH)_2$ "bow-tie" cluster, in which two triangles have a common vertex. Comparing complex **5** with these reported Ni^{II} complexes, we found that all of them have O atoms as bridges and similar Ni···Ni distances and Ni−O−Ni angles.

Crystal Structure of [{$Fe_3(OH)(btapca)_3$]·2DMF·2MeOH] (6)

The molecular structure of complex **6** (Figure 5) is based on an isosceles triangular Fe_3 fragment with a bridging μ_3-OH at the center of the triangle. A C_2 symmetry axis through Fe(2) and the central O(4) atom can be found. Three ligands join three iron atoms through nitrogen atoms from the thiadiazole ring; the bridging μ_3-OH reinforces the trianglar framework. The Fe(1)−Fe(1A), Fe(1)−Fe(2) and Fe(1A)−Fe(2) distances are 3.261, 3.227 and 3.227 Å, respectively, within the range of 2.93−3.65 Å reported in the literature.[26,62] A μ_3-O(4) atom bridges three iron atoms [Fe(1), Fe(1A) and Fe(2)] with Fe−O distances of 1.878(3), 1.878(3) and 1.853(7) Å, respectively. The distance of 1.853(7) Å is typical for $Fe^{3+}-O^{2-}$ bonds in trinuclear (carboxylato)(μ_3-oxo) complexes.[63] A comparison of the μ_3-O−Fe distances in complex **6** with corresponding distances in [$Fe_3O(O_2CC(CH_3)_3]_6(C_5H_5N)_3$] ($\mu_3$-O−$Fe^{3+}$ 1.85, at 295 K),[64] favors the assumption that the oxidation state of the Fe(2) atom is +3. The valence of the other two Fe atoms remains to be +2.

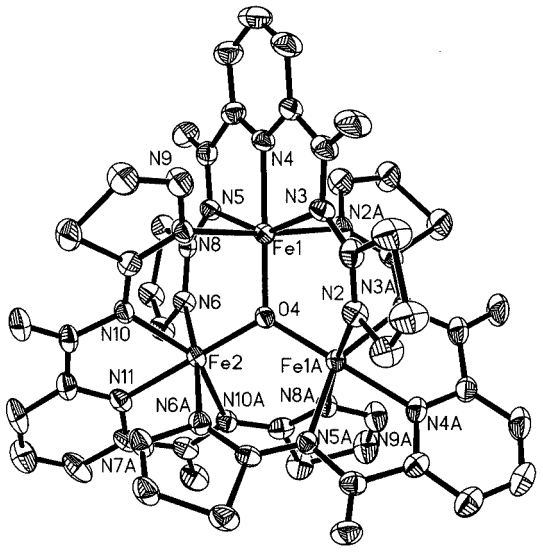

Figure 5. The triangle plane of [{$Fe_3(OH)(btapca)_3$}·2DMF·2MeOH) (**6**), consisting of mixed-valence Fe^{II} and Fe^{III} ions connected together through a μ_3-OH group

Both the Fe^{II} and Fe^{III} ions in **6** have a distorted octahedral geometry with a μ_3-oxygen and five nitrogen atoms. Each Fe center is coordinated simultaneously by three ligands. For example, in the coordination environment of Fe(1), the N(3), N(4) and N(5) donors come from one ligand, N(2A) from the other, and N(8) from the third. μ_3-O(4) and $N(4)_{(py)}$ are at the *trans* positions for all three Fe centers. The four equatorial coordination sites are occupied by N(3), N(4), N(5) and O(4), which are essentially coplanar, with a deviation of 0.0015 Å. Fe(1) is almost in the center of the coordination plane, which deviates from the mean plane by only 0.0019 Å. N(2A) and N(8) from the other two ligands bond to the Fe(1) axial positions to complete the octahedral geometry. The Fe−N distances fall in the range 2.085(9)−2.229(6) Å, which is the typical range for these systems. Three ligands overlap each other like a Chinese knot. Three iron atoms support the triangle knot through a μ_3-oxygen atom. Thus, a closer Fe···Fe contact is found in complex **6**, which benefits the magnetic exchange between the iron centers.

The structure of **6** packs in a large cage-like fashion, in which all the [$Fe_3(OH)(btapca)_3$] units are linked through hydrogen bonding [O(1)···H(11): 2.468 Å; O(3)···H(1): 2.535 Å]. DMF and MeOH solvent molecules occupy the large cages, and the DMF molecules form further hydrogen bonds with [$Fe_3(OH)(btapca)_3$] units [O(5)···H(6): 2.526 Å].

Magnetic Study

The magnetic characterization of **4**−**6** was carried out by measurement of the thermal variation of the paramagnetic susceptibilities χ_p under a magnetic field of 500 G. Because Zn^{II} has no unpaired electrons, complexes **1**−**3** are expected to be diamagnetic.

The magnetic properties of **4** were investigated as described in Figure 6. The χ_pT product exhibits a regular decrease from 3.36 $cm^3·K·mol^{-1}$ at 241 K to 0.97 $cm^3·K·mol^{-1}$ at 5 K, indicating a dominant antiferromagnetic interaction and the spin-orbit coupling of the octahedral Co^{II} centers. Because of this, the μ_{eff} value (5.15 μ_B) of **4** at room temperature is larger than the spin-only value of high-spin cobalt(II) (3.87 μ_B; $\mu_{so} = [4S(S + 1)]^{1/2}$; $S = 3/2$). From 241 to 261 K, χ_pT gradually decreases from 3.36 to 3.24 $cm^3·K·mol^{-1}$, which is an anomaly. This may be due to a transition, possibly associated with the freezing of solvent molecules in the structure and some structural modification. From 261 to 299 K, χ_pT gradually increases from 3.24 to 3.32 $cm^3·K·mol^{-1}$. The close agreement between the experimental and expected μ_{eff} values when the spin momentum and orbital momentum exist independently [5.20 μ_B; $\mu_{1s} = [L(L + 1) + 4S(S + 1)]^{1/2}$; $L = 3$,

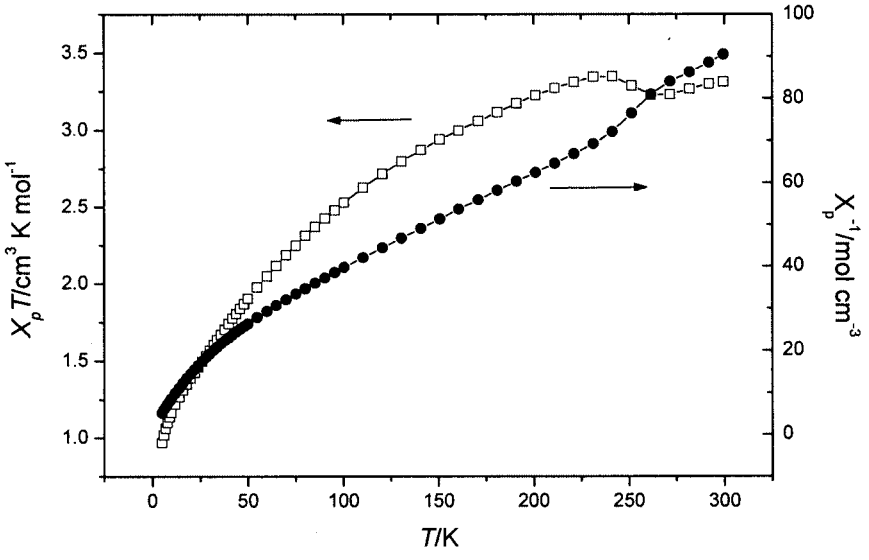

Figure 6. Thermal evolution of χ_pT and χ_p^{-1} of [{$Co_5(OH)_2(btapca)_4$}·4(DMF·MeOH·H_2O) **4**. (χ_p is the paramagnetic susceptibility of **4**)

$S = 3/2$] suggests that there is a contribution of the orbital angular momentum typical for the $^4T_{1g}$ ground state.

The inverse susceptibility varies linearly with temperatures in the experimental regime (85 K $\leq T \leq$ 242 K) and is well fitted in this region by using the Curie−Weiss law, giving $C = 3.71$ cm^3·K·mol^{-1} and $\theta = -37$ K, which further prove the antiferromagnetic exchange. At lower and higher temperatures, χ_p^{-1} shows a characteristic curvature.

In complex **4** there are three kinds of magnetic exchange pathways, namely a Co^{II}-Co^{II} interaction via the μ_3-OH bridge, a magnetic coupling between Co^{II} and Co^{II} through the $N_{(thiazole)}-N_{(thiazole)}$ pathway (5.89 Å), and a Co^{II}-Co^{II} interaction via the $N_{(amide)}-C-N_{(thiazole)}$ bridge (7.077 Å). In consideration of the structural framework, the spin-bearing centers would like to couple antiferromagnetically in triangular or tetrahedral arrays.[65,66] When the unpaired electrons are aligned at 120° and 109° in the triangular and tetrahedral units, respectively, the overall spin vector is equal to zero, as is required for antiferromagnetic coupling.[65] In the spin Co_3O core the Co−O−Co bond angles are about 113°, in accordance with antiferromagnetic behaviour.

The magnetic properties of **5** were studied in the range 5−302 K and the results are given in Figure 7 in the form of χ_pT vs. T and χ_p^{-1} vs. T plots. The variation of χ_p^{-1} is well described by the Curie−Weiss law from 302 to 5 K. The value $C_m = 5.07$ cm^3·K·mol^{-1} and Weiss temperature $\theta = +2$ K are characteristic of a ferromagnetic superexchange. The magnitude of χ_pT increases continuously with decreasing temperature from 5.11 cm^3·K·mol^{-1} (five Ni atoms) at room temp., with a small peak of 5.46 cm^3·K·mol^{-1} at 50 K. From 50 to 44 K, the value of χ_pT decreases slightly from 5.46 to 5.43 cm^3·K·mol^{-1}. After further cooling, the curve rapidly increases to 6.25 cm^3·K·mol^{-1} at 6 K, and then χ_pT begins to decrease. The small peak at around 50 K may be due to molecular oxygen. These results are indicative of the occurrence of ferromagnetic coupling between the metallic centers. The effective magnetic moment at room temperature is 6.4 μ_B, which agrees very well with the spin-only value for five Ni atoms (6.32 μ_B).

In spite of their structural similarity, complex **5** exhibits quite different magnetic behaviour from **4**. We attributed this to the different exchange centers. The metallic centers have superexchange through different pathways, including the btapca ligands and a μ_3-O. Regularly, if the Ni−O−Ni angle is 120°, the complex will exhibit an antiferromagnetic behavior.[67] For face-sharing dioctahedral nickel complexes, Ni−X−Ni bridging angles of (90 ± 14°) are an indication of a ferromagnetic interaction.[29,57,68] The Ni−O−Ni angles in structure **5** are 115.1(5)° and 122.5(2)°, but we can still see a ferromagnetic interaction from the experimental data. Thus, the magnetic exchange through the btapca ligands could dominate even though the pathway through the μ_3-O is much shorter. The low efficiency of these exchange pathways explains the weak ferromagnetic behavior observed for **5**, although the magnetic exchange centers are relatively close to each other. Moreover, the distortions of octahedral geometry around the Ni ion [Ni−N distances ranging from 1.966(7) to 2.276(7) Å with Ni−O lengths of 2.041(6) and 1.704(10) Å] account for the slight weakening of the observed ferromagnetic coupling. Consequently, differences in the bond lengths around Ni ions are directly related to the overlap between the d_{x2-y2} orbital and thus affect the magnitude of the ferromagnetic coupling.

The magnetic behavior of complex **6** is shown in Figure 8 in the form of a χ_pT vs. T plot. χ_pT decreases continuously from 3.14 cm^3·K·mol^{-1} at 302 K to 0.67 cm^3·K·mol^{-1} at 4 K. This behavior is consistent with an antiferromagnetic interaction between the exchange centers. The magnetic susceptibility, plotted as χ_p^{-1} vs. T in Figure 8, follows the Curie−Weiss expression $\chi_p = C/(T - \theta)$ between 110 K and 300 K, with a Curie constant of 3.30 cm^3·K·mol^{-1} and a

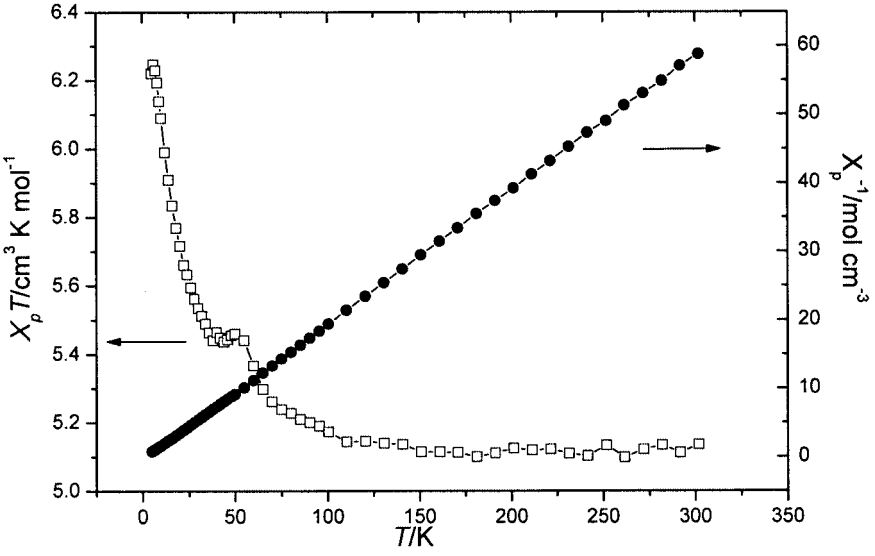

Figure 7. Thermal evolution of χ_pT and χ_p^{-1} of [{$Ni_5(OH)_2(btapca)_4$}·4DMF·MeOH) (**5**); χ_p is the paramagnetic susceptibility of **5**

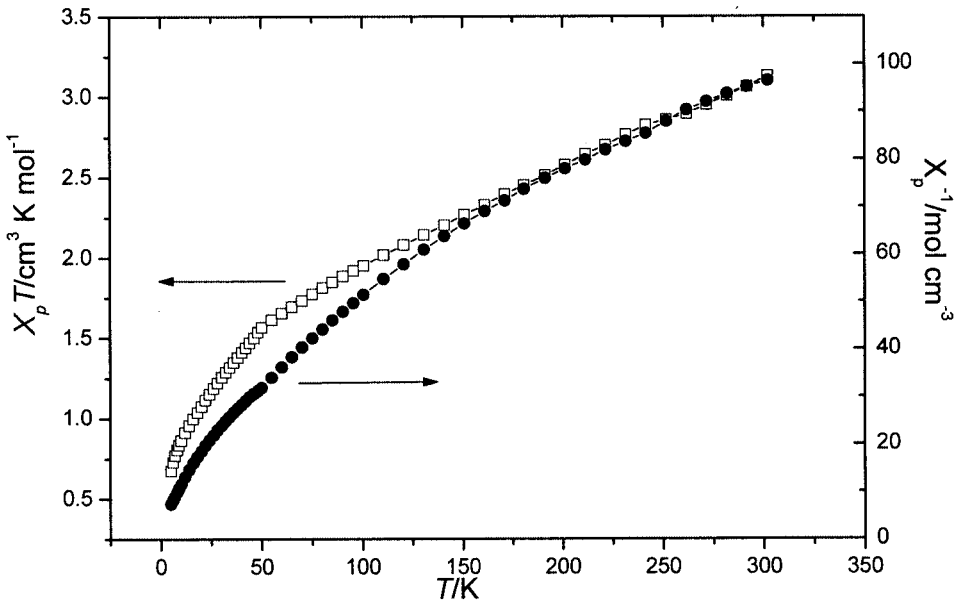

Figure 8. Plots of $\chi_p T$ and χ_p^{-1} vs. T for [{Fe_3(OH)(btapca)$_3$}·2DMF·2MeOH) (**6**); χ_p is the paramagnetic susceptibility of **6**

Curie−Weiss temperature, θ, of −49 K. Below 110 K, the data do not strictly obey the Curie−Weiss law. The effective paramagnetic moment, μ_{eff}, is 5.0 μ_B, indicating a high-spin state for both Fe^{II} (S = 2) and Fe^{III} (S = 5/2) centers. The negative sign for θ suggests an overall antiferromagnetic coupling between the mixed-valence Fe^{II}-Fe^{III} centers.

The magnetic interactions between Fe ions in **6** are achieved mainly through the μ_3-O atom. Although the presence of N−C−N bridges provides an additional exchange pathway (Fe-*N*-C-*N*-Fe about 7.04 Å), they can be neglected due to the shorter Fe−O−Fe bridges (Fe−O−Fe about 3.73 Å). The Fe···Fe distances (about 3.2 Å) differ by only 0.04 Å, and the average Fe−O−Fe angle is 120°. The restricted Fe−O−Fe angle in the iron-$O_{\mu 3}$ plane structures allows magneto-structural correlations. The typical obtuse angle of 120° induces an antiferromagnetic interaction.

The Mössbauer spectrum of complex **6** is similar to that observed for another trimeric, mixed-valent, oxo-centered complex,[69] although it is remarkably different from other trimeric, mixed-valence, oxo-centered complexes.[70,71] The doublets in the Mössbauer spectrum of **6** at room temperature are far from the ratio of 2:1, with isomer shifts and quadrupole splittings of δ_I = 0.27 mm·s^{-1}, ΔE_{QI} = 1.75 mm·s^{-1} and δ_{II} = 0.72 mm·s^{-1}, ΔE_{QII} = 2.63 mm·s^{-1} (Figure 9). This denotes some degree of delocalization (valence detrapping) of the extra electron over the three Fe sites. At room temperature only one doublet is usually found for trimeric, mixed-valent, oxo-centered transition metal complexes due to full delocalization of the "excess" electron over the three iron sites ("valence-detrapped state").[69,70] Complex **6** exhibits a partially valence-delocalized (partially valence-detrapped) state which is similar to the case of a reported Fe^{II}/Fe^{III} complex.[69]

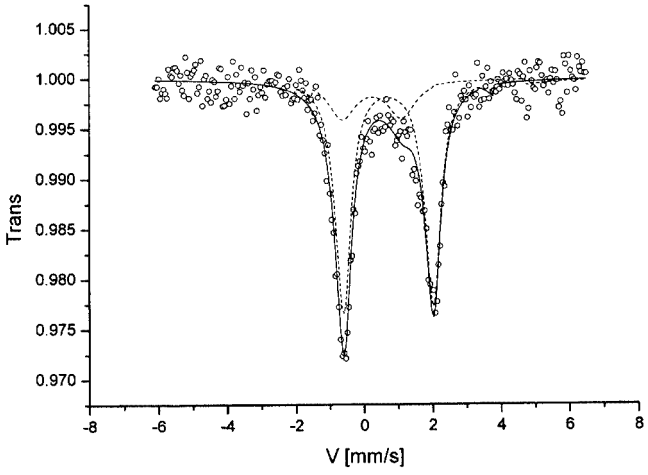

Figure 9. The Mössbauer spectrum of complex [{Fe_3(OH)(btapca)$_3$}·2DMF·2MeOH) (**6**) at room temperature

Conclusion

We have succeeded in obtaining a series of polynuclear complexes constructed from polydentate ligands and different transition-metal salts. The number of metal atoms in these polynuclear complexes ranges from 3 to 6. A μ_3-O atom is a dominant feature in the formation of all these structures. The magnetic behavior of complex **5** shows a ferromagnetic interaction between the Ni^{II} ions, while complexes **4** and **6** both exhibit typical antiferromagnetic exchange between the metal centers.

Experimental Section

General Techniques: 2-Amino-1,3,4-thiadiazole (TBA) was prepared according to a published method.[72] All the other starting chemicals and solvent were commercially available with analytical purity and were used without further purification. A PE 240C Elemental Analyzer was used to perform the elemental analysis. Infrared spectra were measured on a Bruker Tensor 27 infrared spectrophotometer. Fast atom bombardment (FAB) mass spectra were obtained on a Bruker Esquire 3000 mass spectrometer. NMR spectra were obtained using a Bruker DPX-400 spectrometer.

Preparation of *N*,*N*′-Bis(1,3,4-thiadiazol-2-yl)-2,6-pyridinedicarboxamide (btapca): 2,6-Pyridinedicarboxylic acid (1.67 g, 10 mmol) was dissolved in 20 mL of $SOCl_2$. The mixture was refluxed until the white powder dissolved completely. The residual $SOCl_2$ was then removed under reduced pressure. The resulting 2,6-pyridinedicarbonyl dichloride was dissolved in 10 mL of anhydrous pyridine. This pyridine solution of 2-aminodithiazole (2.02 g, 20 mmol) was added dropwise to the 2,6-pyridinedicarbonyl dichloride whilst stirring in an ice bath. Stirring for 4 h resulted in the formation of a white precipitate, which was filtered under reduced pressure and washed with water and methanol. Yield: 2.25 g (70%). $C_{11}H_7N_7O_2S_2$ (333.01): calcd. C 39.64, H 2.12, N 29.41; found C 39.84, H 2.27, N 28.11. ^{1}H NMR (400 MHz, DMSO): δ = 8.39 (q, H), 8.50 (d, 2 H), 9.36 (s, 2 H), 13.73 (d, 2 H) ppm. Positive-ion, ESI-MS: m/z = 333.9 [btapca + H^-].

Synthesis of [{$Zn_6(O)_2$(btapca)$_4$}·3DMF·2H_2O] (1): A DMF solution (5 mL) of btapca (0.1 mmol, 0.0333 g) was added to a methanol solution (5 mL) of $Zn(NO_3)_2$·6H_2O (0.2 mmol, 0.0595 g). The mixture solution was then evaporated to 30% of the original volume at room temperature. Colorless crystals were collected after two weeks with a yield of 30%. IR (KBr pellets): $\tilde{\nu}$ = 3082, 1625, 1667, 1293 cm^{-1}. $C_{53}H_{45}N_{31}O_{15}S_8Zn_6$ (2004.9): calcd. C 31.72, H 2.24, N 21.65; found C 31.51, H 2.31, N 21.22.

Synthesis of [{$Zn_6(O)_2$(btapca)$_4$}·DMF·MeOH·H_2O] (2): A DMF solution (5 mL) of btapca (0.1 mmol, 0.0333 g) was added to a methanol solution (5 mL) of $Zn(OAc)_2$·2H_2O (0.2 mmol, 0.0439 g). The mixture was allowed to stand in air at room temperature for a week resulting in colorless crystals suitable for X-ray diffraction. Yield: 46%. IR (KBr pellets): $\tilde{\nu}$ = 3450, 1626, 1467, 1427, 1376, 1070, 959, 885, 529 cm^{-1}. $C_{48}H_{33}N_{29}O_{13}S_8Zn_6$ (1872.7): calcd. C 30.76, H 1.76, N 21.68; found C 30.95, H 1.58, N 22.01.

Synthesis of [{$Zn_5(OH)_2$(btapca)$_4$}·4DMF·H_2O] (3): A DMF solution (5 mL) of btapca (0.1 mmol, 0.0333 g) was added to a THF solution (5 mL) of ZnI_2 (0.2 mmol, 0.0638 g). A light-yellow solution was obtained after filtration, and this was placed under air. Colorless polyhedral crystals appeared after two weeks. Yield: 25%. IR (KBr pellets): $\tilde{\nu}$ = 3445, 3095, 1639, 1538, 1466, 1444, 1377, 1075, 959, 889 cm^{-1}. $C_{56}H_{52}N_{32}O_{15}S_8Zn_5$ (1996.6): calcd. C 33.66, H 2.60, N 22.44; found C 33.36, H 2.83, N 22.37.

Synthesis of [{$Co_5(OH)_2$(btapca)$_4$}·4DMF·MeOH·H_2O] (4): A DMF solution (5 mL) of btapca (0.1 mmol, 0.0333 g) was added dropwise to a methanol solution (5 mL) of $CoCl_2$·6H_2O (0.2 mmol, 0.0476 g). The resulting red solution produced dark-red crystals suitable for X-ray analysis after four days. Yield: 52%. IR (KBr

Table 1. Crystal data and structure refinement for complexes **1**−**6**

	1	**2**	**3**	**4**	**5**	**6**
Empirical formula	$C_{53}H_{45}N_{31}O_{15}S_8Zn_6$	$C_{48}H_{33}N_{29}O_{13}S_8Zn_6$	$C_{56}H_{52}N_{32}O_{15}S_8Zn_5$	$C_{57}H_{52}Co_5N_{32}O_{17}S_8$	$C_{57}H_{54}N_{32}Ni_5O_{15}S_8$	$C_{41}H_{38}Fe_3N_{23}O_{11}S_6$
Molecular mass	2004.90	1872.73	1996.63	2008.44	1977.35	1388.85
Temperature	291(2) K	291(2) K	291(2) K	291(2) K	293(2) K	291(2) K
Wavelength	0.71073 Å	0.71073 Å	0.71073 Å	0.71073 Å	0.71073 Å	0.71073 Å
Crystal system	triclinic	monoclinic	tetragonal	tetragonal	tetragonal	monoclinic
Space group	$P\bar{1}$	$P2_1/n$	$P4_2/n$	$P4_2/n$	$P4_2/n$	$C2/c$
Unit cell dimensions	a = 14.634(3) Å	a = 13.112(3) Å	a = 14.821(2) Å	a = 14.805(2) Å	a = 14.792(2) Å	a = 15.981(3) Å
	b = 20.794(4) Å	b = 37.227(7) Å	b = 14.821(2) Å	b = 14.805(2) Å	b = 14.792(2) Å	b = 20.199(4) Å
	c = 12.904(3) Å	c = 14.510(3) Å	c = 18.462(4) Å	c = 18.421(4) Å	c = 18.108(4) Å	c = 19.513(4) Å
	α = 99.14(3)°	α = 90°	α = 90°	α = 90°	α = 90°	α = 90°
	β = 96.24(3)°	β = 108.56(3)°	β = 90°	β = 90°	β = 90°	β = 102.47(3)°
	γ = 71.48(3)°	γ = 90°	γ = 90°	γ = 90°	γ = 90°	γ = 90°
Volume	3668.8(13) Å^3	6714(2) Å^3	4055.5(11) Å^3	4037.7(11) Å^3	3962.0(11) Å^3	6150(2) Å^3
Z	2	4	2	2	2	4
Calculated density	1.815 Mg/m^3	1.853 Mg/m^3	1.635 Mg/m^3	1.652 Mg/m^3	1.657 Mg/m^3	1.501 Mg/m^3
Absorption coefficient	2.243 mm^{-1}	2.441 mm^{-1}	1.743 mm^{-1}	1.296 mm^{-1}	1.459 mm^{-1}	0.973 mm^{-1}
F(000)	2016	3744	2020	2034	2016	2832
Index ranges	$0 \le h \le 17$	$-15 \le h \le 14$	$-17 \le h \le 17$	$0 \le h \le 17$	$-17 \le h \le 17$	$-18 \le h \le 14$
	$-21 \le k \le 24$	$-44 \le k \le 43$	$0 \le k \le 17$	$-17 \le k \le 17$	$0 \le k \le 17$	$14 \le k \le 24$
	$-15 \le l \le 15$	$0 \le l \le 17$	$-21 \le l \le 21$	$-21 \le l \le 21$	$-21 \le l \le 20$	$-22 \le l \le 22$
Reflections collected/unique	8194/8194 [R(int) = 0.0000]	15422/9468 [R(int) = 0.0631]	9960/3331 [R(int) = 0.0478]	10257/3115 [R(int) = 0.0463]	10847/3304 [R(int) = 0.0442]	7745/4499 [R(int) = 0.0436]
Refinement method	full-matrix least-squares on F^2	full-matrix least-squares on F^2	full-matrix least-squares on F^2	full-matrix least-squares on F^2	full-matrix least-squares on F^2	full-matrix least-squares on F^2
Data/restraints/parameters	8194/6/934	9468/0/938	3331/5/241	3115/2/272	3304/4/241	4499/0/347
Final R(int) [$I > 2\sigma(I)$]	$R1$ = 0.0773	$R1$ = 0.0556	$R1$ = 0.0768	$R1$ = 0.0580	$R1$ = 0.0832	$R1$ = 0.0737
	$wR2$ = 0.1739	$wR2$ = 0.1003	$wR2$ = 0.1947	$wR2$ = 0.1594	$wR2$ = 0.2615	$wR2$ = 0.2000
Largest diff. peak and hole	1.306 and −0.684 e·Å^{-3}	1.158 and −0.811 e·Å^{-3}	0.979 and −0.438 e·Å^{-3}	0.698 and −0.926 e·Å^{-3}	1.470 and −3.822 e·Å^{-3}	0.810 and −0.570 e·Å^{-3}

pellets): $\tilde{\nu}$ = 3435, 3069, 1709, 1667, 1612, 1437, 1366, 1077, 954, 888 cm^{-1}. $C_{57}H_{52}Co_5N_{32}O_{17}S_8$ (2008.4): calcd. C 34.06, H 2.59, N 22.31; found C 35.22, H 2.27, N 22.65.

Synthesis of [{$Ni_5(OH)_2(btapca)_4$}·4DMF·MeOH] (5): $Ni(NO_3)_2·6H_2O$ (0.1 mmol, 0.0291 g) was dissolved in 5 mL methanol, and a DMF solution (5 mL) of btapca (0.1 mmol, 0.0333 g) was added dropwise to the above solution. The resulting solution was kept at room temperature. Brown crystals suitable for X-ray diffraction were obtained. Yield: 33%. IR (KBr pellets): $\tilde{\nu}$ = 3442, 3075, 1637, 1598, 1465, 1360, 1074, 959, 889 cm^{-1}. $C_{57}H_{54}N_{32}Ni_5O_{15}S_8$ (1977.4): calcd. C 34.59, H 2.73, N 22.66; found C 34.89, H 2.57, N 22.74.

Synthesis of [{$Fe_3(OH)(btapca)_3$}·2DMF·2MeOH] (6). Solutions of btapca (0.1 mmol, 0.0333 g) in DMF and $FeCl_2·4H_2O$ (0.2 mmol, 0.0398 g) in methanol were mixed. Dark-red microcrystals were obtained at room temperature. Yield: 62%. IR (KBr pellets): $\tilde{\nu}$ = 3452, 3079, 1636, 1422, 1358, 1283, 1158, 1043, 959, 888 cm^{-1}.

Table 2. Selected bond lengths (Å) and angles (°) for complexes **1**–**3**

Complex **1**

Zn(1)–O(9)	1.947(9)	Zn(3)–Zn(4)	2.802(2)
Zn(2)–O(9)	1.940(9)	Zn(5)–Zn(6)	3.145(3)
Zn(3)–O(10)	1.979(9)	O(10)–Zn(3)–O(9)	89.5(4)
Zn(3)–O(9)	1.982(9)	O(9)–Zn(4)–O(10)	89.9(4)
Zn(4)–O(9)	1.965(9)	Zn(2)–O(9)–Zn(1)	107.2(4)
Zn(4)–O(10)	1.981(9)	Zn(2)–O(9)–Zn(4)	114.6(5)
Zn(5)–O(10)	1.925(9)	Zn(1)–O(9)–Zn(4)	114.1(4)
Zn(6)–O(10)	1.955(10)	Zn(2)–O(9)–Zn(3)	116.5(4)
Zn(1)–N(9)	2.014(12)	Zn(1)–O(9)–Zn(3)	113.6(5)
Zn(1)–N(3)	2.337(12)	Zn(4)–O(9)–Zn(3)	90.5(4)
Zn(2)–N(6)	2.020(12)	Zn(5)–O(10)–Zn(6)	108.3(4)
Zn(2)–N(12)	2.277(13)	Zn(5)–O(10)–Zn(3)	116.8(5)
Zn(3)–N(27)	1.992(12)	Zn(6)–O(10)–Zn(3)	111.7(4)
Zn(4)–N(13)	1.995(15)	Zn(5)–O(10)–Zn(4)	113.5(4)
Zn(5)–N(19)	2.218(13)	Zn(6)–O(10)–Zn(4)	115.9(5)
Zn(6)–N(24)	2.255(11)	Zn(3)–O(10)–Zn(4)	90.1(4)
Zn(1)–Zn(2)	3.130(3)		

Complex **2**

Zn(1)–O(10)	1.939(5)	Zn(1)–Zn(2)	3.1457(14)
Zn(1)–N(2)	2.021(7)	Zn(3)–Zn(4)	2.8103(13)
Zn(2)–O(10)	1.943(5)	Zn(5)–Zn(6)	3.0927(14)
Zn(2)–N(5)	2.234(6)	Zn(5)–O(9)–Zn(6)	105.7(2)
Zn(3)–O(9)	1.968(5)	Zn(5)–O(9)–Zn(3)	115.0(2)
Zn(3)–N(27)	1.971(6)	Zn(6)–O(9)–Zn(3)	114.9(2)
Zn(3)–O(10)	1.974(5)	Zn(5)–O(9)–Zn(4)	114.7(2)
Zn(3)–N(13)	1.988(6)	Zn(6)–O(9)–Zn(4)	115.8(2)
Zn(4)–O(9)	1.980(5)	Zn(3)–O(9)–Zn(4)	90.8(2)
Zn(4)–O(10)	1.989(5)	Zn(1)–O(10)–Zn(2)	108.2(2)
Zn(4)–N(6)	1.987(6)	Zn(1)–O(10)–Zn(3)	113.6(2)
Zn(4)–N(16)	1.996(6)	Zn(2)–O(10)–Zn(3)	116.2(2)
Zn(5)–O(9)	1.940(5)	Zn(1)–O(10)–Zn(4)	114.2(2)
Zn(5)–N(26)	2.260(6)	Zn(2)–O(10)–Zn(4)	113.7(2)
Zn(6)–O(9)	1.941(5)	Zn(3)–O(10)–Zn(4)	90.3(2)
Zn(6)–N(17)	2.284(6)		

Complex **3**[a]

Zn(1)–O(3)	1.940(11)	O(3)–Zn(1)–N(4)	154.7(4)
Zn(1)–N(4)	2.029(6)	O(3)–Zn(1)–O(3)#1	27.2(5)
Zn(1)–O(3)#1	2.041(12)	N(4)–Zn(1)–O(3)#1	174.2(3)
Zn(1)–N(2)#1	2.128(7)	O(3)–Zn(1)–N(2)#1	107.0(4)
Zn(1)–N(5)	2.167(6)	N(4)–Zn(1)–N(2)#1	96.5(3)
Zn(1)–N(3)	2.215(6)	O(3)#1–Zn(1)–N(2)#1	84.2(3)
Zn(1)–N(7)#2	2.451(9)	O(3)–Zn(1)–N(5)	109.8(3)
Zn(2)–O(3)#3	2.018(8)	N(4)–Zn(1)–N(5)	76.8(3)
Zn(2)–O(3)#1	2.018(8)	O(3)#3–Zn(2)–O(3)#1	161.0(4)
Zn(2)–O(3)#2	2.018(8)	O(3)#3–Zn(2)–O(3)#2	27.0(5)
Zn(2)–O(3)	2.018(8)	O(3)#1–Zn(2)–O(3)#2	161.0(4)
Zn(2)–N(6)	2.293(8)	O(3)#3–Zn(2)–O(3)	161.0(4)
Zn(2)–N(6)#3	2.293(8)	O(3)#1–Zn(2)–O(3)	27.0(5)
Zn(2)–N(6)#2	2.293(8)	O(3)#3–Zn(2)–N(6)	74.5(4)
Zn(2)–N(6)#1	2.293(8)	O(3)#1–Zn(2)–N(6)	86.9(4)
Zn(1)–O(3)–Zn(2)	119.2(6)	Zn(1)–O(3)–Zn(1)#1	110.4(4)
Zn(2)–O(3)–Zn(1)#1	114.5(5)		

[a] Symmetry transformations used to generate equivalent atoms: #1 $-x + 3/2$, $-y + 3/2$, z; #2 y, $-x + 3/2$, $-z + 1/2$; #3 $-y + 3/2$, x, $-z + 1/2$.

Table 3. Selected bond lengths (Å) and angles (°) for complexes **4**–**6**

Complex **4**[a]

Co(1)–O(3)#1	1.998(10)	O(3)#1–Co(1)–O(3)	31.5(4)
Co(1)–O(3)	2.016(9)	O(3)#1–Co(1)–N(4)	169.0(2)
Co(1)–N(4)	2.020(4)	O(3)–Co(1)–N(4)	159.3(3)
Co(1)–N(3)	2.160(4)	O(3)#1–Co(1)–N(3)	94.8(2)
Co(1)–N(5)	2.168(4)	O(3)–Co(1)–N(3)	113.2(2)
Co(1)–N(6)#1	2.197(5)	O(3)–Co(2)–O(3)#3	158.0(3)
Co(1)–N(1)#2	2.262(5)	O(3)–Co(2)–O(3)#2	158.0(3)
Co(2)–O(3)	2.021(7)	O(3)#3–Co(2)–O(3)#2	31.2(4)
Co(2)–O(3)#3	2.021(7)	O(3)–Co(2)–O(3)#1	31.2(4)
Co(2)–O(3)#2	2.021(7)	O(3)#3–Co(2)–O(3)#1	158.0(3)
Co(2)–O(3)#1	2.021(7)	O(3)#2–Co(2)–O(3)#1	158.0(3)
Co(2)–N(2)	2.238(4)	O(3)–Co(2)–N(2)	105.9(2)
Co(2)–N(2)#1	2.238(4)	O(3)#3–Co(2)–N(2)	73.3(3)
Co(2)–N(2)#3	2.238(4)	O(3)#2–Co(2)–N(2)	96.0(3)
Co(2)–N(2)#2	2.238(4)	O(3)#1–Co(2)–N(2)	84.7(2)

Complex **5**[b]

Ni(1)–N(4)	1.966(7)	Ni(2)–N(2)#3	2.276(7)
Ni(1)–O(3)	2.041(6)	Ni(2)–N(2)#1	2.276(7)
Ni(1)–N(5)	2.129(7)	Ni(2)–N(2)	2.276(7)
Ni(1)–N(3)	2.131(7)	O(3)#2–Ni(2)–O(3)	180.000(1)
Ni(1)–N(6)#1	2.140(7)	O(3)#2–Ni(2)–N(2)#2	97.23(17)
Ni(1)–N(1)#2	2.151(7)	O(3)–Ni(2)–N(2)#2	82.77(17)
Ni(2)–O(3)#2	1.704(10)	O(3)#2–Ni(2)–N(2)#3	97.23(17)
Ni(2)–O(3)	1.704(10)	O(3)–Ni(2)–N(2)#3	82.77(17)
Ni(2)–N(2)#2	2.276(7)	N(2)#2–Ni(2)–N(2)#3	165.5(3)
N(4)–Ni(1)–O(3)	175.0(2)	N(4)–Ni(1)–N(6)#1	93.3(3)
N(4)–Ni(1)–N(5)	78.5(3)	O(3)–Ni(1)–N(6)#1	91.7(2)
O(3)–Ni(1)–N(5)	100.8(3)	N(5)–Ni(1)–N(6)#1	93.6(3)
N(4)–Ni(1)–N(1)#2	92.5(3)	N(5)–Ni(1)–N(1)#2	91.1(3)
O(3)–Ni(1)–N(1)#2	82.5(2)	N(3)–Ni(1)–N(1)#2	86.6(3)

Complex **6**[c]

Fe(1)–O(4)	1.878(3)	Fe(2)–O(4)–Fe(1)#1	119.76(18)
Fe(1)–N(4)	2.085(6)	Fe(2)–O(4)–Fe(1)	119.76(18)
Fe(1)–N(5)	2.132(6)	Fe(1)#1–O(4)–Fe(1)	120.5(4)
Fe(1)–N(3)	2.141(6)	O(4)–Fe(1)–N(4)	179.6(2)
Fe(1)–N(8)	2.226(6)	O(4)–Fe(1)–N(5)	104.1(2)
Fe(1)–N(2)#1	2.229(6)	N(4)–Fe(1)–N(5)	76.0(2)
Fe(2)–O(4)	1.853(7)	O(4)–Fe(1)–N(2)#1	91.8(2)
Fe(2)–N(11)	2.085(9)	N(4)–Fe(1)–N(2)#1	88.5(2)
Fe(2)–N(10)	2.131(6)	N(5)–Fe(1)–N(2)#1	90.3(2)
Fe(2)–N(10)#1	2.131(6)	N(3)–Fe(1)–N(2)#1	89.0(3)
Fe(2)–N(6)	2.209(5)	O(4)–Fe(2)–N(10)	104.31(18)
Fe(2)–N(6)#1	2.209(5)	N(11)–Fe(2)–N(10)	75.69(18)
O(4)–Fe(1)#1	1.878(3)	O(4)–Fe(2)–N(10)#1	104.31(18)
O(4)–Fe(2)–N(11)	180.000(1)		

[a] Symmetry transformations used to generate equivalent atoms: #1 $-x + 5/2$, $-y + 5/2$, z; #2 y, $-x + 5/2$, $-z - 1/2$; #3 $-y + 5/2$, x, $-z - 1/2$; #4 y, $-x + 5/2$, $-z + 1/2$. [b] Symmetry transformations used to generate equivalent atoms: #1 $-x + 3/2$, $-y + 3/2$, z; #2 y, $-x + 3/2$, $-z + 1/2$; #3 $-y + 3/2$, x, $-z + 1/2$; #4 $-y + 3/2$, x, $-z + 3/2$; #5 y, $-x + 3/2$, $-z + 3/2$. [c] Symmetry transformations used to generate equivalent atoms: #1 $-x$, y, $-z + 1/2$; #2 $-x + 1/2$, $-y + 3/2$, $-z$.

$C_{41}H_{38}Fe_3N_{23}O_{11}S_6$ (1388.9): calcd. C 35.42, H 2.74, N 23.18; found C 35.12, H 2.80, N 23.52.

Magnetic Studies: Temperature-dependent magnetic-susceptibility measurements on powdered solid samples were carried out on a SQUID magnetometer (MPMS Quantum Design) over the temperature range 5−300 K. The magnetic field applied was 500 G. The observed susceptibility data were corrected for underlying diamagnetism by using Pascal's constants.[73]

Mössbauer Measurement: Mössbauer spectra were obtained in transmission mode using a ^{57}Co source in a Rh matrix. 64.8 mg of the samples was used and the spectra were measured on an Austin S-600 Mössbauer spectrometer. The spectra were recorded at room temperature at a speed of 6 mm/s. The source was kept at room temperature. The hyperfine field parameters were obtained by fitting the raw data with Lorentz-shaped lines using the program "Mössbauer spectra for Fitting" by Prof. Z. X. Xu (Material Physics and Chemistry Department, University of Science and Technology Beijing). The hyperfine field data are referenced against α-Fe.

X-ray Crystallographic Study: The diffraction intensities of prismatic crystals of complexes **1**, **2**, **3**, **4**, **5** and **6** were collected with graphite-monochromated Mo-K_α radiation (λ = 0.71073 Å) using a Rigaku R-AXIS-IV diffractometer at 291(2) K to a maximum 2θ value of 50°. The unit-cell parameters were determined from the reflections collected on oscillation frames and were then refined. The data were corrected for Lorentz and polarization effects. The structures were solved by direct methods with SHELXS-97[74] and subsequent Fourier-difference synthesis and refined by the full-matrix least-squares method on F^2 with SHELXL-97.[75] All non-hydrogen atoms, except atoms in disordered parts, were refined anisotropically; hydrogen atoms were placed at calculated positions and refined as riding atoms with isotropic displacement parameters. Crystal data and structure refinement details for the seven compounds are given in Table 1. Selected bond lengths and angles of complexes **1**−**6** are listed in Table 2 and 3.
CCDC-212348 (for **1**), -212349 (for **2**), -212351 (for **3**), -212350 (for **4**), -212352 (for **5**) and -212354 (for **6**) contain the supplementary crystallographic data for this paper. These data can be obtained free of charge at www.ccdc.cam.ac.uk/conts/retrieving.html [or from the Cambridge Crystallographic Data Centre, 12 Union Road, Cambridge CB2 1EZ, UK; Fax: +44-1223-336033; E-mail: deposit@ccdc.cam.ac.uk].

Acknowledgments

This work was supported by the National Natural Science Foundation of China (Nos. 20001006 and 20371042), the Excellent Young Teachers Program In Higher Education Institute and Henan Province.

[1] G. M. Whitesides, J. P. Mathias, C. T. Seto, *Science* **1991**, *254*, 1312−1319.
[2] G. F. Swiegers, T. J. Malefetse, *Chem. Rev.* **2000**, *100*, 3483−3537.
[3] [3a] S. S. Sun, A. J. Lee, *J. Am. Chem. Soc.* **2000**, *122*, 8956−8967. [3b] D. S. Lawrence, T. Jiang, M. Levett, *Chem. Rev.* **1995**, *95*, 2229−2260.
[4] Y. B. Dong, M. D. Smith, H. C. Z. Loye, *Angew. Chem. Int. Ed.* **2000**, *39*, 4271−4273.
[5] L. K. Thompson, L. Zhao, Z. Xu, D. O. Miller, W. M. Reiff, *Inorg. Chem.* **2003**, *42*, 128−139.
[6] E. Colacio, M. Ghazi, H. Stoeckli-Evans, F. Lloret, J. M. Moreno, C. Pérez, *Inorg. Chem.* **2001**, *40*, 4876−4883.
[7] *Monographs in Supramolecular Chemistry* (Ed.: J. F. Stoddart), Royal Society of Chemistry, Cambridge, UK, **1989, 1991, 1994−1996**; vols. 1−6.
[8] D. B. Amabilino, J. F. Stoddart, *Chem. Rev.* **1995**, *95*, 2725−2828.
[9] D. B. Amabilino, M. Asakawa, P. R. Ashton, R. Ballardini, V. Balzani, M. Belohradský, A. Credi, M. Higuchi, F. M. Raymo, T. Shimizu, J. F. Stoddart, M. Venturi, K. Yase, *New J. Chem.* **1998**, *22*, 959−972.
[10] S. Leininger, B. Olenyuk, P. J. Stang, *Chem. Rev.* **2000**, *100*, 853−908.
[11] [11a] K. S. Jeong, Y. L. Cho, J. U. Song, H. Y. Chang, M. G. Choi, *J. Am. Chem. Soc.* **1998**, *120*, 10982−10983. [11b] F. A. Cotton, L. M. Daniels, C. Lin, C. A. Murillo, *Chem. Commun.* **1999**, 841−842. [11c] S. M. Woessner, J. B. Helms, J. F. Houlis, B. P. Sullivan, *Inorg. Chem.* **1999**, *38*, 4380−4381. [11d] S. S. Sun, A. S. Silva, I. M. Brinn, A. J. Lees, *Inorg. Chem.* **2000**, *39*, 1344−1345.
[12] [12a] R. V. Slone, K. D. Benksrein, S. Bélanger, J. T. Hupp, I. A. Guzei, A. L. Rheingold, *Coord. Chem. Rev.* **1998**, *171*, 221−243. [12b] S. Bélanger, J. T. Hupp, C. L. Stern, R. V. Slone, D. F. Watson, T. G. Carrell, *J. Am. Chem. Soc.* **1999**, *121*, 557−563. [12c] S. Bélanger, J. T. Hupp, *Angew. Chem. Int. Ed.* **1999**, *38*, 2222−2224.
[13] [13a] Y. Zhang, S. Wang, G. D. Enright, S. R. Breeze, *J. Am. Chem. Soc.* **1998**, *120*, 9398−9399. [13b] K. Onitsuka, S. Yamamoto, S. Takahashi, *Angew. Chem. Int. Ed.* **1999**, *38*, 174−176.
[14] Y. L. Cho, H. Uh, S. Y. Chang, H. Y. Chang, M. G. Choi, I. Shin, K. S. Jeong, *J. Am. Chem. Soc.* **2001**, *123*, 1258−1259.
[15] [15a] M. Fujita, *Chem. Soc. Rev.* **1998**, *27*, 417−425. [15b] D. L. Caulder, K. N. Raymond, *Acc. Chem. Res.* **1999**, *32*, 975−982.
[16] [16a] R. D. Schnebeck, E. Freisinger, F. Glahé, B. Lippert, *J. Am. Chem. Soc.* **2000**, *122*, 1381−1390. [16b] F. Würthner, A. Sautter, *Chem. Commun.* **2000**, 445−446. [16c] A. J. Blake, N. R. Champness, A. N. Khlobystov, S. Parsons, M. Schröder, *Angew. Chem. Int. Ed.* **2000**, *39*, 2317−2320. [16d] K. D. Benkstein, J. T. Hupp, C. L. Stern, *Angew. Chem. Int. Ed.* **2000**, *39*, 2891−2893.
[17] [17a] N. Takeda, K. Umemoto, K. Yamaguchi, M. Fujita, *Nature* **1999**, *398*, 794−796. [17b] B. Olenuyuk, J. A. Whiteford, A. Fechtenkötter, P. J. Stang, *Nature* **1999**, *398*, 796−799. [17c] A. Ikeda, M. Yoshimura, H. Udzu, C. Fukuhara, S. Shinkai, *J. Am. Chem. Soc.* **1999**, *121*, 4296−4297. [17d] N. P. Tatjana, M. Scherer, K. N. Raymond, *Angew. Chem. Int. Ed.* **2000**, *39*, 1239−1242. [17e] M. Yoshizawa, T. Kusukawa, M. Fujita, K. Yamaguchi, *J. Am. Chem. Soc.* **2000**, *122*, 6311−6312.
[18] E. C. Sãnudo, V. A. Grillo, M. J. Knapp, J. C. Bollinger, J. C. Huffman, D. N. Hendrickson, G. Christou, *Inorg. Chem.* **2002**, *41*, 2441−2450.
[19] [19a] M. Soler, P. Artus, K. Folting, J. C. Huffman, D. N. Hendrickson, G. Christou, *Inorg. Chem.* **2001**, *40*, 4902−4912. [19b] R. Sessoli, H.-L. Tsai, A. R. Schake, S. Wang, J. B. Vincent, K. Folting, D. Gatteschi, G. Christou, D. N. Hendrickson, *J. Am. Chem. Soc.* **1993**, *115*, 1804−1816. [19c] S. Wang, K. Folting, W. E. Streib, E. A. Schmitt, J. K. McCusker, D. N. Hendrickson, G. Christou, *Angew. Chem. Int. Ed. Engl.* **1991**, *30*, 305−306. [19d] J. K. McCusker, J. B. Vincent, E. A. Schmitt, M. L. Mino, K. Shin, D. K. Coggin, P. M. Hagen, J. C. Huffman, G. Christou, D. N. Hendrickson, *J. Am. Chem. Soc.* **1991**, *113*, 3012−3021.
[20] [20a] A. Bino, M. Ardon, D. Lee, B. Spingler, S. J. Lippard, *J. Am. Chem. Soc.* **2002**, *124*, 4578−4579. [20b] E. Y. Tshuva, D. Lee, W. Bu, S. J. Lippard, *J. Am. Chem. Soc.* **2002**, *124*, 2416−2417. [20c] S. C. Burdette, S. J. Lippard, *Coord. Chem. Rev.* **2001**, *216−217*, 333−361. [20d] S. C. Burdette, S. J. Lippard, *PNAS Perspect.* **2003**, *100*, 3605−3610. [20e] D. Lee, S. J. Lippard, *J. Am. Chem. Soc.* **2001**, *123*, 4611−4612.
[21] A. Kamiyama, T. Noguchi, T. Kajiwara, T. Ito, *Inorg. Chem.* **2002**, *41*, 507−512.
[22] V. Pavlishchuk, F. Birkelbach, T. Weyhermüller, K. Wieghardt, P. Chaudhuri, *Inorg. Chem.* **2002**, *41*, 4405−4416.

[23] L. K. Thompson, *Coord. Chem. Rev.* **2002**, *233−234*, 193−206.
[24] T. L. Borgne, E. Rivière, J. Marrot, P. Thuéry, J. J. Girerd, M. Ephritikhine, *Chem. Eur. J.* **2002**, *8*, 774−783.
[25] J. M. Clemente-Juan, C. Mackiewicz, M. Verelst, F. Dahan, A. Bousseksou, Y. Sanakis, J. P. Tuchagues, *Inorg. Chem.* **2002**, *41*, 1478−1491.
[26] K. S. Gavrilenko, A. Vértes, G. Vanko, L. F. Kiss, A. W. Addison, T. Weyhermüller, V. V. Pavlishchuk, *Eur. J. Inorg. Chem.* **2002**, 3347−3355.
[27] P. E. Kruger, B. Moubaraki, G. D. Fallon, K. S. Murray, *J. Chem. Soc., Dalton Trans.* **2000**, 713−718.
[28] Z. E. Serna, M. G. Barandika, R. Cortés, M. K. Urtiaga, G. E. Barberis, T. Rojo, *J. Chem. Soc., Dalton Trans.* **2000**, 29−34.
[29] M. Du, X. H. Bu, Y. M. Guo, L. Zhang, D. Z. Liao, J. Ribas, *Chem. Commun.* **2002**, 1478−1479.
[30] M. J. Hossain, M. Yamasaki, M. Mikuriya, A. Kuribayashi, H. Sakiyama, *Inorg. Chem.* **2002**, *41*, 4058−4062.
[31] X. R. Meng, Y. L. Song, H. W. Hou, Y. T. Fan, G. Li, Y. Zhu, *Inorg. Chem.* **2003**, *42*, 1306−1315.
[32] H. W. Hou, X. R. Meng, Y. L. Song, Y. T. Fan, Y. Zhu, H. J. Lu, C. X. Du, W. H. Shao, *Inorg. Chem.* **2003**, *42*, 4068−4075.
[33] H. W. Hou, Y. L. Song, H. Xu, Y. L. Wei, Y. T. Fan, Y. Zhu, L. K. Li, C. X. Du, *Macromolecules* **2003**, *36*, 999−1008.
[34] H. W. Hou, Y. L. Wei, Y. L. Song, Y. Zhu, L. K. Li, Y. T. Fan, *J. Mater. Chem.* **2002**, *12*, 838−843.
[35] H. W. Hou, G. Li, L. K. Li, Y. Zhu, X. R. Meng, Y. T. Fan, *Inorg. Chem.* **2003**, *42*, 428−435.
[36] G. Li, Y. L. Song, H. W. Hou, L. K. Li, Y. T. Fan, Y. Zhu, X. R. Meng, L. W. Mi, *Inorg. Chem.* **2003**, *42*, 913−920.
[37] B. H. Ye, X. Y. Li, L. D. Williams, X. M. Chen, *Inorg. Chem.* **2002**, *41*, 6426−6431.
[38] V. Chandrasekhar, S. Kingsley, B. Rhatigan, M. K. Lam, A. L. Rheingold, *Inorg. Chem.* **2002**, *41*, 1030−1032.
[39] W. N. Lipscomb, N. Sträter, *Chem. Rev.* **1996**, *96*, 2375−2434.
[40] D. E. Wilcox, *Chem. Rev.* **1996**, *96*, 2435−2458.
[41] N. Sträter, W. N. Lipscomb, T. Klabunde, B. Krebs, *Angew. Chem. Int. Ed. Engl.* **1996**, *35*, 2024−2055.
[42] X. M. Chen, Y. X. Tong, T. C. W. Mak, *Inorg. Chem.* **1994**, *33*, 4586−4588.
[43] P. Chaudhuri, C. Stckheim, K. Wieghardt, W. Deck, R. Gregorzik, H. Vahrenkamp, B. Nuber, J. Weiss, *Inorg. Chem.* **1992**, *331*, 1451−1457.
[44] I. S. Müller, R. Robson, *Angew. Chem. Int. Ed.* **2000**, *39*, 4357−4359.
[45] M. Dey, C. P. Rao, P. Saarenketon, K. Rissanen, E. Kolehmainen, *Eur. J. Inorg. Chem.* **2002**, 2207−2215.
[46] D. Walther, T. Döhler, N. Theyssen, H. Görls, *Eur. J. Inorg. Chem.* **2001**, 2049−2060.
[47] O. P. Anderson, A. L. Cour, A. Dodd, A. D. Garrett, M. Wicholas, *Inorg. Chem.* **2003**, *42*, 122−127.
[48] S. O. H. Gutschke, D. J. Price, A. K. Powell, P. T. Wood, *Eur. J. Inorg. Chem.* **2001**, 2739−2741.
[49] D. Katerina, D. B. Angelica, E. C. Thomas, R. L. Arnold, C. George, *Chem. Commun.* **2001**, 1284−1285.
[50] X. Fan, R. Cao, M. Hong, W. Su, D. Sun, *J. Chem. Soc., Dalton Trans.* **2001**, 2961−2962.
[51] T. A. Chesnokova, E. V. Zhezlova, K. A. Kornev, Y. V. Fedotova, L. N. Mushtina, G. A. Domrachev, *J. Organomet. Chem.* **2002**, *642*, 20−31.
[52] K. Yamamoto, S. Nakazawa, A. Matsufuji, T. Taguchi, *J. Chem. Soc., Dalton Trans.* **2001**, 251−258.
[53] V. Schwartz, R. Prins, X. Wang, W. M. H. Sachtler, *J. Phys. Chem. B* **2002**, *106*, 7210−7217.
[54] Z. Q. Xu, L. K. Thompson, V. A. Milway, L. Zhao, T. Kelly, D. O. Miller, *Inorg. Chem.* **2003**, *42*, 2950−2959.
[55] L. K. Thompson, C. J. Matthews, L. Zhao, Z. Xu, D. O. Miller, C. Wilson, M. A. Leech, J. A. K. Howard, S. L. Heath, A. G. Whitteker, R. E. P. Winpenny, *J. Solid State Chem.* **2001**, *159*, 308−320.
[56] H. Carlsson, M. Haukka, E. Nordlander, *Inorg. Chem.* **2002**, *41*, 4981−4983.
[57] B. Kersting, G. Steinfeld, D. Siebert, *Chem. Eur. J.* **2001**, *7*, 4253−4258.
[58] A. Escuer, M. Font-Bardía, E. Peñalba, N. Sanz, X. Solans, R. Vicente, *J. Chem. Soc., Dalton Trans.* **1999**, 3115−3119.
[59] A. Escuer, C. J. Harding, Y. Dussart, J. Nelson, V. McKee, R. Vicente, *J. Chem. Soc., Dalton Trans.* **1999**, 223−227.
[60] I. Castro, M. L. Calatayud, J. Sletten, F. Lloret, M. Julve, *J. Chem. Soc., Dalton Trans.* **1997**, 811−817.
[61] C. S. Campos-Fernández, R. Clérac, J. M. Koomen, D. H. Russell, K. R. Dunbar, *J. Am. Chem. Soc.* **2001**, *123*, 773−774.
[62] D. B. D. Amico, D. Boschi, F. Calderazzo, S. Ianelli, L. Labella, F. Marchetti, G. Pelizzi, E. G. F. Quadrelli, *Inorg. Chim. Acta* **2000**, *300−302*, 882−891.
[63] S. G. Shova, I. G. Kadelnik, M. Gdanec, Yu. A. Simonove, T. K. Zhovmir, V. M. Meriacre, G. Filotti, K. I. Turte, *Zh. Strukt. Khim.* **1998**, *39*, 917−933.
[64] C. Wilson, B. B. Iversen, J. Overgaard, F. K. Larsen, G. Wu, S. P. Palii, G. A. Timco, N. V. Gerbeleu, *J. Am. Chem. Soc.* **2000**, *122*, 11370−11379.
[65] S. R. Marshall, A. L. Rheingold, L. N. Dawe, W. W. Shum, C. Kitamura, J. S. Miller, *Inorg. Chem.* **2002**, *41*, 3599−3601.
[66] J. E. Greedan, *J. Mater. Chem.* **2001**, *11*, 37−53.
[67] B. N. Figgis, E. S. Kucharski, M. Vrtis, *J. Am. Chem. Soc.* **1993**, *115*, 176−181.
[68] K. K. Nanda, L. K. Thompson, J. N. Bridson, K. Nag, *J. Chem. Soc., Chem. Commun.* **1994**, 1337−1338 and references cited therein.
[69] V. Coropceanu, V. Schünemann, C. Ober, M. Gerdan, A. X. Trautwein, J. Köhler, R. W. Saalfrank, *Inorg. Chim. Acta* **2000**, *300−302*, 875−881.
[70] R. D. Cannon, R. P. White, *Prog. Inorg. Chem.* **1988**, *36*, 195−298, and references cited therein.
[71] C. C. Wu, H. G. Jang, A. L. Rheingold, P. Gütlich, D. N. Hendrickson, *Inorg. Chem.* **1996**, *35*, 4137−4147.
[72] R. Q. Huang, H. L. Wang, J. Zhou, *Synthesis of Organic Intermediates*, Chemistry Engineering Publisher, Peking, **1996**, p.134.
[73] R. L. Carlin, *Magnetochemistry*, Springer, Berlin, Heidelberg, New York, Tokyo, **1986**.
[74] G. M. Sheldrick, *Acta Crystallogr., Sect. A* **1990**, *46*, 467−473.
[75] G. M. Sheldrick, *SHELXL-97, Program for the Refinement of Crystal Structures*, University of Göttingen, **1997**.

Received February 11, 2004
Early View Article
Published Online July 22, 2004

